JOURNAL OF Materials CHEMISTRY

Syntheses and characterization of $Co_2(4,4'\text{-bipy})_2(V_4O_{12})$, $Co(pz)(VO_3)_2$ and $Co_2(2\text{-pzc})(H_2O)(VO_3)_3$ (4,4′-bipy = 4,4′-bipyridine, pz = pyrazine, 2-pzc = 2-pyrazinecarboxylate)

Li-Min Zheng,[a]† **Xiqu Wang,**[a] **Yongsheng Wang**[b] **and Allan J. Jacobson***[a]

[a] *Department of Chemistry, University of Houston, Houston TX 77204, USA. E-mail: ajjacob@uh.edu; Fax: 713-7432787; Tel: 713-7432785*
[b] *Department of Physics, University of Houston, Houston TX 77204, USA*

Received 13th November 2000, Accepted 16th January 2001
First published as an Advance Article on the web 1st March 2001

By using different organic ligands, three new inorganic–organic hybrid compounds of cobalt vanadium oxide have been synthesized hydrothermally: $Co_2(4,4'\text{-bipy})_2(V_4O_{12})$ **1**, $Co(pz)(VO_3)_2$ **2** and $Co_2(2\text{-pzc})(H_2O)(VO_3)_3$ **3**, where 4,4′-bipy = 4,4′-bipyridine, pz = pyrazine, 2-pzc = 2-pyrazinecarboxylate. Crystal data: **1**, triclinic, space group $P\text{-}\bar{1}$, $a = 8.164(2)$, $b = 8.587(2)$, $c = 10.162(2)$ Å, $\alpha = 87.04(3)$, $\beta = 75.72(3)$, $\gamma = 75.02(3)°$; **2**, orthorhombic, space group *Pnna*, $a = 10.2793(8)$, $b = 11.5639(9)$, $c = 7.4822(6)$ Å; **3**, orthorhombic, space group $Pna2_1$, $a = 15.253(1)$, $b = 8.2554(7)$, $c = 10.6784(9)$ Å. Compound **1** contains $\{CoV_2O_6\}$ layers cross-linked by 4,4′-bipyridine ligands. Compounds **2** and **3** are three-dimensional frameworks containing both infinite metavanadate chains and either {Co(pz)} or $\{Co_2(2\text{-pzc})\}$ chains. The magnetic properties of **1**–**3** are reported.

Introduction

The solution and solid-state chemistries of oxovanadium(v) compounds are of interest because of their structural richness and varied physical properties. The equilibria in solution between polyoxovanadium(v) species are complex. The crystallization of particular species is strongly dependent upon the solution properties such as pH, ionic strength, temperature, and the specific counterion.[1,2] In so-called 'metavanadate' aqueous solutions (pH *ca.* 6.5–8), the major constituents are the cyclic tetramer $V_4O_{12}{}^{4-}$ and the pentamer $V_5O_{15}{}^{5-}$ although infinite metavanadate chain compounds are crystallized from solution.[2]

Recent studies of the hydrothermal syntheses of inorganic–organic hybrid materials based on vanadium oxides have shown that the tetrameric anion in the 'metavanadate' aqueous solution may be 'trapped' by coordination components. Examples reported previously include the molecular compounds $Zn_2(bipy)_4V_4O_{12}$, $Zn_2(phen)_4V_4O_{12}$,[3] the layer compound $Ni(dien)V_2O_6$,[4] and the three-dimensional compound $Co_2(3,3'\text{-bipy})_4(V_4O_{12})$.[5] But in the compounds $Cu(NH_3)_2V_2O_6$,[6] $Cu(en)V_2O_6$, $Cu(bipy)V_2O_6$, $Cu(bipy)_2V_2O_6$,[7] $Cu(dien)V_2O_6{\cdot}H_2O$,[4] $Cu(dpa)VO_3$[8] and $Cu_3(trz)_2(VO_3)_4$,[9] infinite metavanadate chains are observed. The related compound $[(bipy)_2Zn]_2[V_6O_{17}]$[10] contains a two-dimensional vanadium(v) oxide layer built up from corner-sharing metavanadate chains. Related compounds containing mixed valence vanadium oxide layers have also been reported.[10–12]

In the crystallization of the vanadium(v) oxide species as a tetrameric anion, an infinite chain or even as layers in the above examples, the specific ligand and the second metal ion play very important roles. For example, all of the ligated copper vanadate compounds reported so far contain metavanadate chains, no matter whether a mono-, bi- or tri-dentate ligand is used. Because of our interest in synthesizing metal–organic coordination polymers stabilized by metavanadate chains as a route to useful inorganic–organic materials with high thermal stability, we have investigated the use of different organic bridging ligands in the cobalt vanadate system. Here we report the syntheses, structures and characterization of three new compounds: $Co_2(4,4'\text{-bipy})_2(V_4O_{12})$ **1**, $Co(pz)(VO_3)_2$ **2** and $Co_2(2\text{-pzc})(H_2O)(VO_3)_3$ **3**, where 4,4′-bipy = 4,4′-bipyridine, pz = pyrazine, 2-pzc = 2-pyrazinecarboxylate. The magnetic properties of **1**–**3** are also reported.

Experimental

Materials and methods

All the starting materials were reagent grade and used as purchased. The infrared spectra were recorded on a Galaxy FTIR 5000 series spectrometer with pressed KBr pellets. Thermal analyses were performed in air with a heating rate of 5 °C min^{-1} on a TGA V5.1A DuPont 2100 instrument. The powder XRD patterns were recorded on a Scintag XDS 2000 diffractometer. Magnetic susceptibility data for **1**–**3** were obtained on polycrystalline samples (**1**: 9.4 mg, **2**: 23 mg, **3**: 29.2 mg) from 2 to 300 K in a magnetic field of 5 kG using a SQUID magnetometer. Diamagnetic corrections were estimated from Pascal's constants.[13]

Synthesis of $Co_2(4,4'\text{-bipy})_2(V_4O_{12})$ 1

The hydrothermal reaction of a mixture of $Co(NO_3)_2{\cdot}6H_2O$ (0.5 mmol, 0.1474 g), NH_4VO_3 (0.7 mmol, 0.0805 g), 4,4′-bipyridine (0.5 mmol, 0.0796 g) and H_2O (8 mL) at 160 °C for 1 d results in the dark-red needles of the compound **1** as a major phase, together with a very small amount of an unidentified black microcrystalline phase. Yield: *ca.* 66% based on vanadium. IR (KBr, cm^{-1}): 1609m, 1535w, 1489w, 1411w, 1321w, 1219w, 1074w, 1012w, 961m, 936m, 909s, 855w, 818s, 795s, 731w, 635w, 571w, 511w.

---

†On leave from State Key Laboratory of Coordination Chemistry, Coordination Chemistry Institute, Nanjing University, Nanjing 210093, P. R. China.

DOI: 10.1039/b009091n

Synthesis of $Co(pz)(VO_3)_2$ 2

Compound **2** was obtained by the hydrothermal reaction of a mixture of $Co(NO_3)_2 \cdot 6H_2O$ (0.5 mmol, 0.1473 g), NH_4VO_3 (0.5 mmol, 0.0597 g), pyrazine (1.0 mmol, 0.0808 g) and H_2O (8 mL) at 160 °C for 1 d. Dark-red crystals were formed as a single phase, judged by powder X-ray diffraction. Yield: 90% based on vanadium. IR (KBr, cm^{-1}): 1414m, 1385vw, 1163m, 1119m, 1088w, 1057m, 912s, 818m, 789w, 758m, 638s, 546w, 475m.

Synthesis of $Co_2(2\text{-pzc})(H_2O)(VO_3)_3$ 3

A mixture of $Co(2\text{-pzc})_2(H_2O)_2$ (0.1712 g, 0.5 mmol), NH_4VO_3 (0.0884 g, 0.75 mmol) and H_2O (8 mL) was heated at 160 °C for 2 d to produce a pure phase of brown, flat needles. Yield: 71% based on vanadium. IR (KBr, cm^{-1}): 3509m, 3380m, 1528m, 1580m, 1532vw, 1472w, 1433m, 1377m, 1238vw, 1192m, 1161w, 1076m, 1042m, 955m, 932m, 907s, 891s, 837m, 820m, 774s, 733m, 625s, 536m, 480m.

X-Ray crystallographic analysis

Single crystals of dimension $0.27 \times 0.05 \times 0.03$ mm for **1**, $0.20 \times 0.04 \times 0.04$ mm for **2** and $0.18 \times 0.07 \times 0.015$ mm for **3** were used for structural determination on a Siemens SMART platform diffractometer equipped with a 1 K CCD area detector using graphite-monochromatized MoKα radiation at 295 K for **1**–**3**. For each phase a hemisphere of data (1271 frames at 5 cm detector distance) was collected using a narrow-frame method with scan widths of 0.30° in ω and an exposure time of 30 s $frame^{-1}$ for **1**–**2** and 35 s $frame^{-1}$ for **3**. The first 50 frames were re-measured at the end of data collection to monitor instrument and crystal stability, and the maximum correction applied on the intensities was $<1\%$. The data were integrated using the Siemens SAINT program,[14] with the intensities corrected for Lorentz factor, polarization, air absorption, and absorption due to variation in the path length through the detector faceplate. Absorption corrections were made using the program SADABS.[15] The structures were solved by direct methods and refined using SHELXTL.[16] All non-hydrogen positions were derived by direct methods and refined anisotropically in the final refinements. The hydrogen atoms for **1**–**3** were located from difference maps. All H atoms were allowed to ride on their respective parent atoms and refined isotropically. Crystallographic and refinement details are summarized in Table 1. Atomic coordinates for **1**–**3** are listed in Tables 2–4, and selected bond lengths and angles in Tables 5–7.

CCDC reference numbers 152985–152987. See http://www.rsc.org/suppdata/jm/b0/b009091n/ for crystallographic data in CIF or other electronic format.

Results and discussion

Crystal structures

The structure of $Co_2(4,4'\text{-bipy})_2(V_4O_{12})$ **1** can be described as a three-dimensional structure formed from inorganic $\{Co_2V_4O_{12}\}_n$ layers that are cross-linked by 4,4′-bipyridine molecules [Fig. 1(a)]. Within the inorganic layer, $[V_4O_{12}]^{4-}$ tetramers are isolated from each other. The tetramer shares O(1), O(3) and O(6) atoms with six cobalt trigonal bipyramids [Fig. 1(b) and Fig. 2] with the O(5) atom terminal [V(2)–O(5) 1.616(2) Å]. Each Co atom is five-coordinated and has a distorted trigonal bipyramidal geometry. The three equatorial positions are occupied by the O(1), O(3) and O(6) atoms from three $[V_4O_{12}]^{4-}$ tetramers (the sum of bond angles on the basal plane is 360°). The two axial positions are occupied by N atoms from two equivalent 4,4′-bipyridine ligands [N(1)–Co(1)–N(2C) 179.3(1)°]. The Co–N [2.128(2), 2.142(2) Å] and Co–O [1.971(2)–1.989(2) Å] distances are normal. The 4,4′-bipyridine acts as a bridging ligand. Hence, the pure inorganic $\{Co_2V_4O_{12}\}_n$ layers are interconnected by Co(4,4′-bipy) chains, forming a three-dimensional pillared, layered structure. The shortest Co···Co distance within the inorganic layer is 4.582 Å, and that between the layers across the 4,4′-bipyridine bridge is 11.358 Å.

The structure of $Co(pz)(VO_3)_2$ **2** is built up from corner-sharing metavanadate chains running along the *b*-axis and $\{Co(pz)\}_n$ chains. As shown in Fig. 3, the two nitrogen atoms from two equivalent pyrazine ligands occupy the axial positions of each cobalt octahedron [Co–N 2.148(2) Å]. The four equatorial sites are occupied by four oxygen atoms from three $\{VO_3\}_n$ chains [Co–O 2.047(2), 2.094(2) Å]. There are two types of $\{Co(pz)\}_n$ chains in the lattice, oriented in the [011] and [01−1] directions, respectively. The flexible $\{VO_3\}_n$ chains link the $\{Co(pz)\}_n$ chains to form a three-dimensional framework structure (Fig. 4). The shortest Co···Co distance over the VO_4 bridge is 6.357 Å, and that across the pyrazine bridge is 7.047 Å.

Compound $Co_2(2\text{-pzc})(H_2O)(VO_3)_3$ **3** also has a framework structure. It is composed of infinite chains $\{Co_2(2\text{-pzc})\}_n$ and

Table 1 Crystal data for **1**–**3**

Compound	**1**	**2**	**3**
Formula	$C_{10}H_8CoN_2O_6V_2$	$C_4H_4CoN_2O_6V_2$	$C_5H_5Co_2N_2O_{12}V_3$
Formula weight	412.99	336.9	555.79
Crystal system	Triclinic	Orthorhombic	Orthorhombic
Space group	$P\text{-}\bar{1}$	*Pnna*	$Pna2_1$
a/Å	8.164(2)	10.279(1)	15.253(1)
b/Å	8.587(2)	11.564(1)	8.255(1)
c/Å	10.162(2)	7.482(1)	10.678(1)
α/°	87.04(3)		
β/°	75.72(3)		
γ/°	75.02(3)		
V/Å^3, Z	666.9(2), 2	889.4(1), 4	1344.6(2), 4
D_c/g cm^{-3}	2.057	2.516	2.745
μ/cm^{-1}	26.28	39.09	44.95
Reflections collected	4241	4967	6226
Independent reflections [$I > 2\sigma(I)$]	2930 (2593) [$R_{int} = 0.0155$]	1072 (934) [$R_{int} = 0.0355$]	2203 (1783) [$R_{int} = 0.0425$]
Parameters	214	77	224
Goodness-of-fit on F^2	1.029	1.058	1.040
R_1,[a] wR_2[b] [$I > 2\sigma(I)$]	0.0327, 0.0784	0.0273, 0.0596	0.0265, 0.0576
All data	0.0401, 0.0822	0.0360, 0.0626	0.0322, 0.0592
Extinction coefficient	0.0011(6)	0.0006(3)	
$\Delta\rho_{max}$, $\Delta\rho_{min}$ /e Å^{-3}	0.988, −0.432	0.400, −0.364	0.497, −0.374

[a] $R_1 = \Sigma||F_o| - |F_c||/\Sigma|F_o|$. [b] $wR_2 = [\Sigma w(F_o^2 - F_c^2)^2/\Sigma w(F_o^2)^2]^{1/2}$.

Table 2 Atomic coordinates and equivalent isotropic displacement parameters (Å^2) for **1**. $U_{(eq)}$ is defined as one third of the trace of the orthogonalized U_{ij} tensor

Atom	x	y	z	$U_{(eq)}$
Co(1)	0.3443(1)	−0.1612(1)	−0.0582(1)	0.013(1)
V(1)	0.2685(1)	0.2728(1)	−0.0301(1)	0.014(1)
V(2)	−0.1277(1)	0.4103(1)	0.1973(1)	0.013(1)
N(1)	0.1672(3)	−0.1643(3)	0.1341(2)	0.016(1)
N(2)	−0.4785(3)	−0.1549(3)	0.7483(2)	0.018(1)
O(1)	0.2815(3)	0.0784(2)	−0.0478(2)	0.023(1)
O(2)	0.1038(3)	0.3554(3)	0.1147(2)	0.022(1)
O(3)	0.4587(3)	0.2928(3)	−0.0120(2)	0.023(1)
O(4)	0.2195(3)	0.3774(2)	−0.1770(2)	0.020(1)
O(5)	−0.1530(3)	0.3712(3)	0.3572(2)	0.025(1)
O(6)	−0.2299(3)	0.3029(3)	0.1293(2)	0.022(1)
C(1)	0.0374(4)	−0.0332(4)	0.1804(3)	0.021(1)
C(2)	−0.0875(4)	−0.0288(4)	0.3786(3)	0.017(1)
C(4)	0.0509(4)	−0.3039(4)	0.3318(3)	0.021(1)
C(5)	0.1730(4)	−0.2980(4)	0.2101(3)	0.020(1)
C(6)	−0.2182(4)	−0.1645(4)	0.5066(3)	0.018(1)
C(7)	−0.2850(5)	−0.0274(4)	0.5899(3)	0.029(1)
C(8)	−0.4117(5)	−0.0278(4)	0.7073(3)	0.029(1)
C(9)	−0.4157(4)	−0.2867(4)	0.6669(3)	0.026(1)
C(10)	−0.2882(4)	−0.2962(4)	0.5474(3)	0.024(1)

Table 3 Atomic coordinates and equivalent isotropic displacement parameters (Å^2) for **2**. $U_{(eq)}$ is defined as one third of the trace of the orthogonalized U_{ij} tensor

Atom	x	y	z	$U_{(eq)}$
V(1)	0.2249(1)	0.3538(1)	0.0981(1)	0.011(1)
Co(1)	−0.0727(1)	0.2500	0.2500	0.010(1)
O(1)	0.0672(2)	0.3294(2)	0.0878(2)	0.017(1)
O(2)	0.2872(2)	0.3318(2)	−0.1022(2)	0.020(1)
O(3)	0.2500	0.5000	0.1705(4)	0.023(1)
O(4)	0.2927(3)	0.2500	0.2500	0.019(1)
N(1)	−0.0438(2)	0.1006(2)	0.0839(3)	0.016(1)
C(1)	0.0188(3)	0.1038(2)	−0.0719(4)	0.021(1)
C(2)	−0.0618(3)	−0.0045(2)	0.1565(4)	0.020(1)

Table 4 Atomic coordinates and equivalent isotropic displacement parameters (Å^2) for **3**. $U_{(eq)}$ is defined as one third of the trace of the orthogonalized U_{ij} tensor

Atom	x	y	z	$U_{(eq)}$
Co(1)	0.1352(1)	0.5615(1)	0.3244(1)	0.015(1)
Co(2)	0.3877(1)	0.4353(1)	0.2317(1)	0.014(1)
V(1)	0.1066(1)	0.1970(1)	0.1613(1)	0.013(1)
V(2)	0.3004(1)	0.0459(1)	0.1437(1)	0.013(1)
V(3)	0.4173(1)	−0.1816(1)	0.3700(1)	0.013(1)
O(1)	0.3341(3)	0.5721(5)	0.0651(4)	0.022(1)
O(2)	0.2582(2)	0.5408(5)	0.2397(4)	0.019(1)
O(3)	0.0068(3)	0.1201(5)	0.1616(5)	0.022(1)
O(4)	0.1316(3)	0.3067(5)	0.0220(4)	0.023(1)
O(5)	0.1171(3)	0.3204(5)	0.2805(4)	0.022(1)
O(6)	0.1844(3)	0.0319(5)	0.1743(4)	0.021(1)
O(7)	0.3311(3)	0.2365(5)	0.1549(5)	0.024(1)
O(8)	0.3234(3)	−0.0155(5)	0.0012(4)	0.021(1)
O(9)	0.3498(3)	−0.0789(5)	0.2603(4)	0.025(1)
O(10)	0.4379(3)	−0.3646(5)	0.3166(4)	0.021(1)
O(11)	0.5095(3)	−0.0809(5)	0.3826(4)	0.022(1)
O(1W)	0.1610(3)	0.8008(6)	0.3762(5)	0.033(1)
N(1)	0.1108(3)	0.6514(6)	0.1349(5)	0.014(1)
N(2)	0.1128(3)	0.8066(7)	−0.0948(5)	0.016(1)
C(1)	0.0370(4)	0.7131(8)	0.0857(6)	0.019(2)
C(2)	0.0399(4)	0.7933(9)	−0.0283(7)	0.023(2)
C(3)	0.1857(4)	0.7389(8)	−0.0483(6)	0.016(2)
C(4)	0.1840(4)	0.6629(7)	0.0678(5)	0.013(1)
C(5)	0.2648(4)	0.5902(7)	0.1246(6)	0.019(2)

Table 5 Selected bond lengths (Å) and angles (°) for **1**

Co(1)–O(6)#1	1.971(2)	Co(1)–O(3)#2	1.979(2)
Co(1)–O(1)	1.989(2)	Co(1)–N(1)	2.128(2)
Co(1)–N(2)#3	2.142(2)	V(1)–O(3)	1.660(2)
V(1)–O(1)	1.662(2)	V(1)–O(2)	1.765(2)
V(1)–O(4)	1.779(2)	V(2)–O(5)	1.616(2)
V(2)–O(6)	1.665(2)	V(2)–O(4)#4	1.805(2)
V(2)–O(2)	1.816(2)		
O(6)#1–Co(1)–O(3)#2	109.92(9)	O(6)#1–Co(1)–O(1)	128.75(9)
O(3)#2–Co(1)–O(1)	121.31(10)	O(6)#1–Co(1)–N(1)	88.41(9)
O(3)#2–Co(1)–N(1)	91.13(9)	O(1)–Co(1)–N(1)	89.30(9)
O(6)#1–Co(1)–N(2)#3	92.01(9)	O(3)#2–Co(1)–N(2)#3	89.27(9)
O(1)–Co(1)–N(2)#3	89.99(10)	N(1)–Co(1)–N(2)#3	179.29(9)
O(3)–V(1)–O(1)	109.07(12)	O(3)–V(1)–O(2)	108.89(11)
O(1)–V(1)–O(2)	110.49(11)	O(3)–V(1)–O(4)	109.64(11)
O(1)–V(1)–O(4)	109.30(11)	O(2)–V(1)–O(4)	109.44(10)
O(5)–V(2)–O(6)	109.20(12)	O(5)–V(2)–O(4)#4	109.15(11)
O(6)–V(2)–O(4)#4	109.72(10)	O(5)–V(2)–O(2)	109.06(11)
O(6)–V(2)–O(2)	109.42(10)	O(4)#4–V(2)–O(2)	110.27(10)
V(1)–O(1)–Co(1)	168.04(14)	V(1)–O(2)–V(2)	147.46(13)
V(1)–O(3)–Co(1)#2	136.78(13)	V(1)–O(4)–V(2)#4	129.13(12)
V(2)–O(6)–Co(1)#1	175.34(14)	C(1)–N(1)–Co(1)	120.3(2)
C(5)–N(1)–Co(1)	122.3(2)	C(8)–N(2)–Co(1)#5	122.7(2)
C(9)–N(2)–Co(1)#5	120.4(2)	C(10)–C(6)–C(3)	122.1(3)

Symmetry transformations used to generate equivalent atoms: #1 $-x,-y,-z$; #2 $-x+1,-y,-z$; #3 $x+1,y,z-1$; #4 $-x,-y+1,-z$; #5 $x-1,y,z+1$.

Table 6 Selected bond lengths (Å) and angles (°) for **2**

V(1)–O(1)	1.647(2)	V(1)–O(2)	1.650(2)
V(1)–O(4)	1.7937(11)	V(1)–O(3)	1.7942(9)
Co(1)–O(2)	2.047(2) 2*x*	Co(1)–O(1)	2.094(2) 2*x*
Co(1)–N(1)	2.148(2) 2*x*		
O(1)–V(1)–O(2)	108.27(9)	O(1)–V(1)–O(4)	107.31(10)
O(2)–V(1)–O(4)	108.79(8)	O(1)–V(1)–O(3)	108.45(7)
O(2)–V(1)–O(3)	111.32(10)	O(4)–V(1)–O(3)	112.54(8)
O(2)#1–Co(1)–O(2)#2	90.62(11)	O(2)#1–Co(1)–O(1)	88.13(7) 2*x*
O(2)#2–Co(1)–O(1)	177.21(7) 2*x*	O(1)#3–Co(1)–O(1)	93.23(10)
O(1)–Co(1)–N(1)#3	83.54(8) 2*x*	O(2)#1–Co(1)–N(1)	99.00(8) 2*x*
O(2)#2–Co(1)–N(1)	92.18(8) 2*x*	C(2)–N(1)–Co(1)	118.3(2)
O(1)–Co(1)–N(1)	85.56(8) 2*x*	N(1)#3–Co(1)–N(1)	164.11(12)
V(1)–O(1)–Co(1)	136.39(10)	V(1)–O(2)–Co(1)#4	146.60(11)
V(1)–O(3)–V(1)#5	144.8(2)	V(1)–O(4)–V(1)#3	134.3(2)
C(1)–N(1)–Co(1)	123.4(2)		

Symmetry transformations used to generate equivalent atoms: #1 $x-1/2,y,-z$; #2 $x-1/2,-y+1/2,z+1/2$; #3 $x,-y+1/2,-z+1/2$; #4 $x+1/2,y,-z$; #5 $-x+1/2,-y+1,z$.

metavanadate chains $\{VO_3\}_n$. Within the $\{Co_2(2\text{-pzc})\}_n$ chain, pairs of Co(1) and Co(2) octahedra share one carboxylate oxygen atom O(2) (Fig. 5 and 6). The Co(1)···Co(2) distance in the dimer is 4.110 Å. The other carboxylate oxygen atom O(1) is also coordinated to Co(2) and as a result the Co(2) octahedron is strongly distorted. The O(1)–Co(2)–O(2) angle is 59.9(2)°. The Co dimers are bridged by the 2-pyrazinecarboxylate ligand in a zigzag fashion (Fig. 6). The Co(1)···Co(2) distance across the pyrazine bridge is 7.051 Å. The three oxygen atoms coordinated to each Co are shared with three VO_4 groups. The other three positions of the cobalt octahedra are occupied by N(1), O(2) and O(1W) for Co(1), and O(1), O(2) and N(2) for Co(2). The Co–N and Co–O bond lengths are 2.136(5)–2.186(5) and 2.019(4)–2.260(4) Å, respectively. Each $\{Co_2(2\text{-pzc})\}_n$ chain is embraced by two metavanadate chains, forming a $\{Co_2(2\text{-pzc})(VO_3)_3\}_n$ triple chain. The triple chains are further connected to each other by sharing O(3) and O(11) to form the three-dimensional framework (Fig. 7). The shortest Co···Co distance across a VO_4 unit is 5.662 Å.

The infinite metavanadate chain can be crystallized together with either $\{Co(pz)\}_n$ or $\{Co_2(2\text{-pzc})\}_n$ chains. When 4,4′-bipyridine replaces pyrazine, the V_4O_{12} tetramers are formed. The V_4O_{12} tetramer is also found in compound $Co_2(3,3'\text{-bipy})_2(V_4O_{12})$.[5] Clearly, the size of the bridging ligand influences the different vanadium oxide polymeric units in

Table 7 Selected bond lengths (Å) and angles (°) for **3**

Co(1)–O(11)#1	2.022(4)	Co(1)–O(5)	2.063(4)
Co(1)–O(2)	2.089(4)	Co(1)–O(1W)	2.089(5)
Co(1)–O(8)#2	2.090(4)	Co(1)–N(1)	2.187(5)
Co(2)–O(3)#3	2.017(4)	Co(2)–O(7)	2.028(4)
Co(2)–O(10)#4	2.034(4)	Co(2)–N(2)#5	2.136(5)
Co(2)–O(2)	2.161(4)	Co(2)–O(1)	2.260(4)
V(1)–O(5)	1.638(4)	V(1)–O(3)	1.650(4)
V(1)–O(4)	1.783(4)	V(1)–O(6)	1.811(4)
V(2)–O(8)	1.641(4)	V(2)–O(7)	1.646(4)
V(2)–O(9)	1.784(4)	V(2)–O(6)	1.803(4)
V(3)–O(11)	1.639(4)	V(3)–O(10)	1.646(4)
V(3)–O(9)	1.774(4)	V(3)–O(4)#5	1.790(4)
O(11)#1–Co(1)–O(5)	91.1(2)	O(11)#1–Co(1)–O(2)	172.2(2)
O(5)–Co(1)–O(2)	86.7(2)	O(11)#1–Co(1)–O(1W)	91.3(2)
O(5)–Co(1)–O(1W)	176.1(2)	O(2)–Co(1)–O(1W)	91.3(2)
O(11)#1–Co(1)–O(8)#2	91.9(2)	O(5)–Co(1)–O(8)#2	87.3(2)
O(2)–Co(1)–O(8)#2	95.5(2)	O(1W)–Co(1)–O(8)#2	89.5(2)
O(11)#1–Co(1)–N(1)	95.5(2)	O(5)–Co(1)–N(1)	95.4(2)
O(2)–Co(1)–N(1)	77.3(2)	O(1W)–Co(1)–N(1)	87.5(2)
O(8)#2–Co(1)–N(1)	172.1(2)	O(3)#3–Co(2)–O(7)	92.9(2)
O(3)#3–Co(2)–O(10)#4	90.6(2)	O(7)–Co(2)–O(10)#4	176.3(2)
O(3)#3–Co(2)–N(2)#5	102.2(2)	O(7)–Co(2)–N(2)#5	86.9(2)
O(10)#4–Co(2)–N(2)#5	91.1(2)	O(3)#3–Co(2)–O(2)	158.4(2)
O(7)–Co(2)–O(2)	87.3(2)	O(10)#4–Co(2)–O(2)	90.0(2)
N(2)#5–Co(2)–O(2)	99.4(2)	O(3)#3–Co(2)–O(1)	98.5(2)
O(7)–Co(2)–O(1)	86.1(2)	O(10)#4–Co(2)–O(1)	94.7(2)
N(2)#5–Co(2)–O(1)	158.5(2)	O(2)–Co(2)–O(1)	60.0(2)
C(5)–O(1)–Co(2)	88.0(4)	C(5)–O(2)–Co(1)	117.0(4)
C(5)–O(2)–Co(2)	91.0(4)	Co(1)–O(2)–Co(2)	150.6(2)
V(1)–O(3)–Co(2)#1	156.8(3)	V(1)–O(5)–Co(1)	142.2(3)
V(2)–O(7)–Co(2)	157.6(3)	V(2)–O(8)–Co(1)#7	143.9(3)
V(3)–O(10)–Co(2)#8	145.9(2)	V(3)–O(11)–Co(1)#3	146.0(3)
C(4)–N(1)–Co(1)	112.3(4)	C(1)–N(1)–Co(1)	129.3(4)
C(2)–N(2)–Co(2)#6	120.3(5)	C(3)–N(2)–Co(2)#6	122.1(4)

Symmetry transformations used to generate equivalent atoms: #1 $x-1/2,-y+1/2,z$; #2 $-x+1/2,y+1/2,z+1/2$; #3 $x+1/2,-y+1/2,z$; #4 $x,y+1,z$; #5 $-x+1/2,y-1/2,z+1/2$; #6 $-x+1/2,y+1/2,z-1/2$; #7 $-x+1/2,y-1/2,z-1/2$; #8 $x,y-1,z$.

the compounds **1**–**3**. The Co···Co distances across the pyrazine bridge (7.047 Å for **2** and 7.051 Å for **3**, respectively) are much shorter than that over the 4,4′-bipyridine bridge (11.358 Å) in **1**. The metavanadate chain can coexist with the cobalt–pyrazine infinite chain.

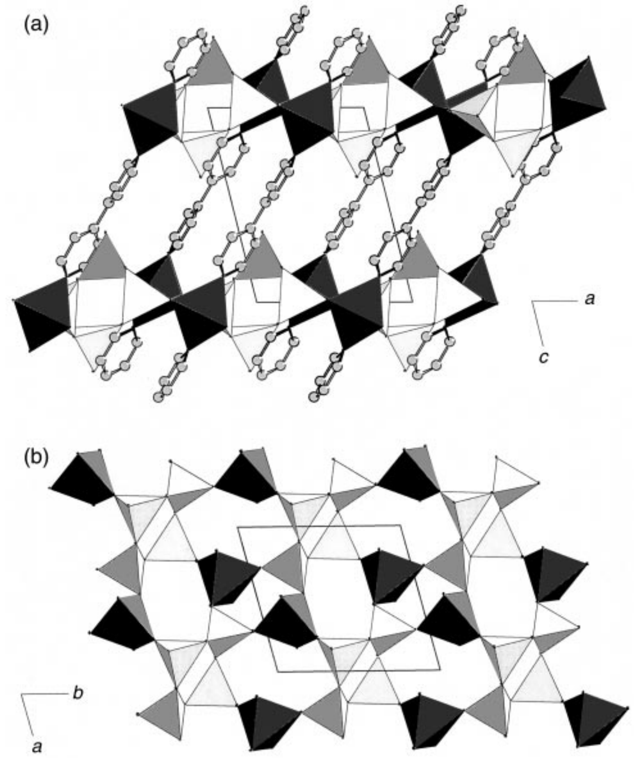

Fig. 1 (a) View of the structure of **1** along the [010] direction, and (b) the inorganic layer in **1**. All H atoms are omitted for clarity.

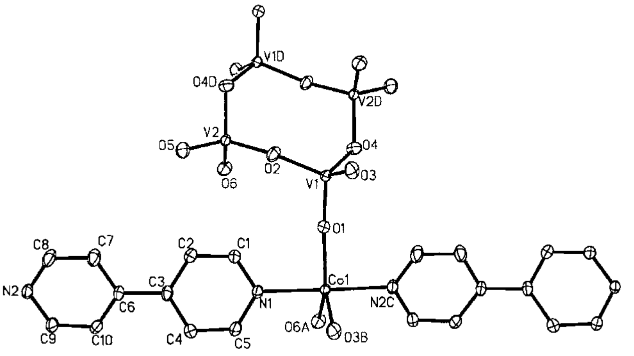

Fig. 2 Fragment of the structure of **1** with the atomic labeling scheme (thermal ellipsoids at 50% probability).

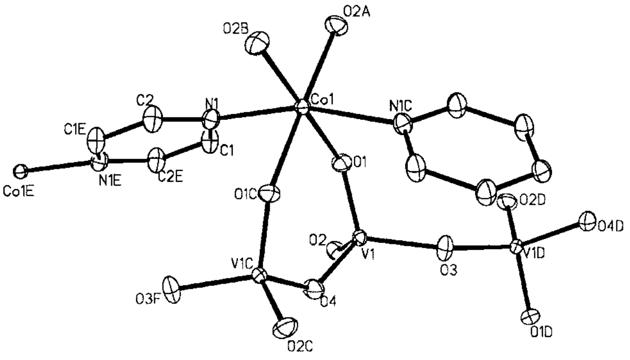

Fig. 3 Fragment of the structure of **2** with atomic labeling scheme (thermal ellipsoids at 50% probability).

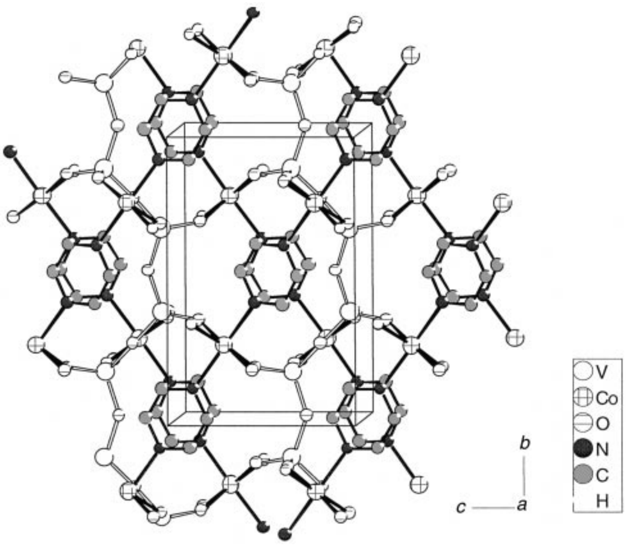

Fig. 4 View of the structure of **2** approximately along [100] direction. All H atoms are omitted for clarity.

Thermal stability and magnetic properties

Thermal analyses have been performed in air for **1**–**3** between room temperature and 600 °C. All three show a one-step, sharp decomposition process, with the maximum rate at 410, 406 and 430 °C, respectively. The weight losses for **1** and **2** are in agreement with the removal of the organic ligands [Found (calcd.): 37.1 (37.8)% for **1**; 23.0 (23.7)% for **2**]. The weight loss

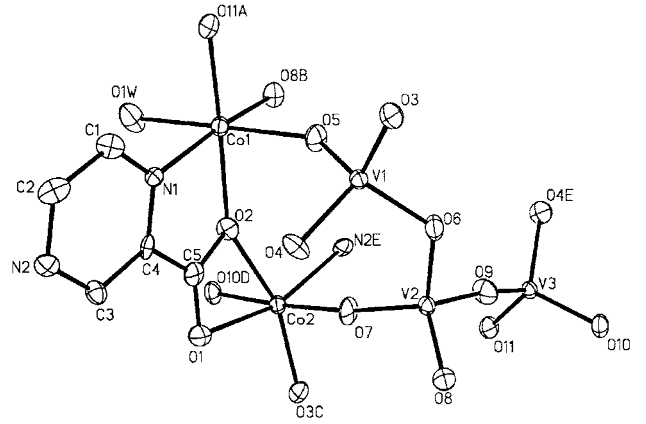

Fig. 5 Fragment of the structure of **3** with atomic labeling scheme (thermal ellipsoids at 50% probability).

Fig. 6 Polyhedral representation of $\{Co_2(2\text{-pzc})(H_2O)\}_n$ chain.

for **3** (23.9%) agrees well with the removal of one water molecule and the organic ligand assuming that the residue is $2CoO{\cdot}1.5V_2O_5$ (calcd. 23.9%). The residues in each case could not be unambiguously identified. Compared with other metal 4,4′-bipyridine, pyrazine and 2-pyrazinecarboxylate polymers,[17,18] the thermal stabilities of **1**–**3** are significantly higher. It is interesting to note that the coordinated water molecule in **3** is unusually stable on heating.

The temperature dependent magnetic susceptibilities of **1**–**3** have been measured in the range 300–2 K. At 300 K, the magnetic moments (μ_{eff}) per cobalt(II) atom, determined from the equation $\mu_{eff}=2.828(\chi_m T)^{1/2}$, are 3.77 μ_B for **1**, 4.60 μ_B for **2** and 4.58 μ_B for **3**. The values of **2** and **3** are much higher than that expected for an isolated $S=3/2$ ion ($\mu_{eff}=3.87$ μ_B), due to the contribution from orbital angular momentum at high temperatures. Fig. 8 shows the magnetic behavior of **1**. The maximum appearing at *ca.* 36 K in the χ_m *vs.* T plot indicates an antiferromagnetic interaction between cobalt(II) ions. The structure **1** contains $\{Co_2V_4O_{12}\}_n$ layers interconnected by Co(4,4′-bipy) chains. As the shortest Co···Co distance across the 4,4′-bipyridine bridge is 11.358 Å, the magnetic exchange coupling through the 4,4′-bipyridine bridge is expected to be very weak. The overall antiferromagnetic interaction should be mainly attributed to the superexchange coupling within the inorganic layer. It is noticed that the shortest Co···Co distance within the inorganic layer in **1** is 4.582 Å, much shorter than those in **2** and **3** across the VO_4 bridges. The magnetic data were thus analyzed according to an isotropic dimer model for $S=3/2$ ions.[19] The theoretical fitting resulted in parameters $g=2.17$, $J=-17.4\ cm^{-1}$, the paramagnetic impurity $\rho=0.0497$. If an inter-dimer interaction (θ) is included, the fit is improved with the parameters $g=2.15$, $J=-13.7\ cm^{-1}$, $\theta=-7.7$ K, $\rho=0.058$ (Fig. 8).

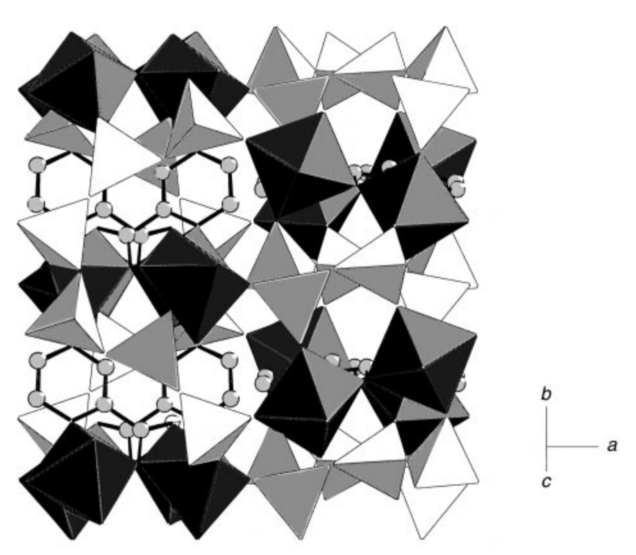

Fig. 7 Packing diagram of the structure of **3** viewed along [011] direction.

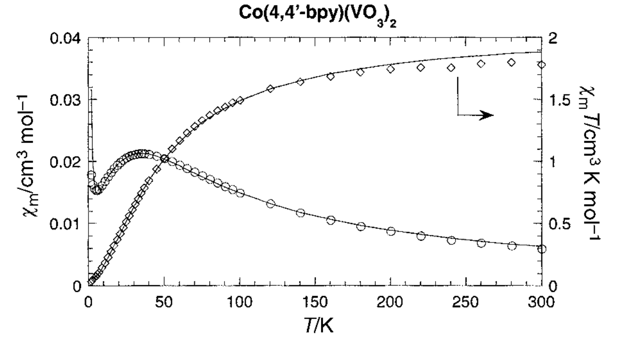

Fig. 8 χ_m and $\chi_m T$ *vs.* T for **1**. The open symbols are the experimental data, the solid lines are the fits.

The magnetic behavior of **2** is shown in Fig. 9. Above 70 K, the data can be fit to the Curie–Weiss expression giving $g=2.46$, $\theta=-20.2$ K, which indicates an antiferromagnetic interaction. In **2** the pyrazine-bridged $\{Co(pz)\}_n$ chain is isolated by diamagnetic metavanadate chains with the shortest Co···Co distance across VO_4 units being 6.375 Å. The magnetic exchange coupling is, therefore, propagated through pyrazine

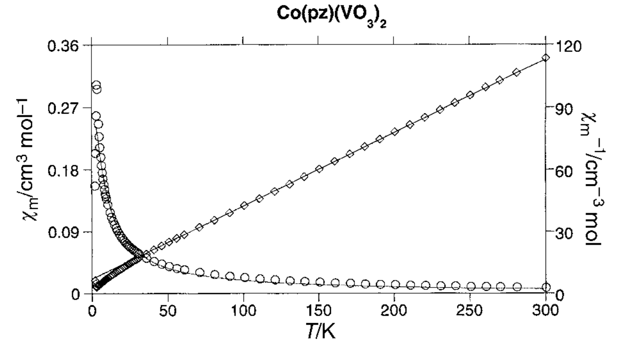

Fig. 9 χ_m *vs.* T and χ_m^{-1} *vs.* T for **2**. The open symbols are the experimental data, the solid lines are the fits.

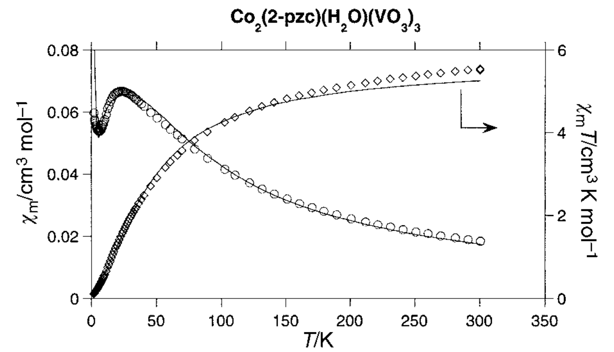

Fig. 10 χ_m and $\chi_m T$ *vs.* T for **3**. The open symbols are the experimental data, the solid lines are the fits.

bridges. The data were analyzed by a Fisher chain model[13] which is valid for large spin values. The theoretical fit, shown as the solid line in Fig. 9, results in the parameters $g=2.06$ and $J=-0.9\ \mathrm{cm}^{-1}$. The small J value is consistent with the other pyrazine-bridged compounds[20] where only very weak antiferromagnetic interactions occur between the magnetic centers.

For **3**, a maximum is observed at 22 K in the χ_m *vs.* T plot (Fig. 10), indicating an antiferromagnetic exchange coupling. This exchange is mainly attributed to the paramagnetic $\{\mathrm{Co_2(2\text{-}pzc)}\}_n$ chain which contains corner sharing dimers of cobalt octahedra. The data were analyzed by an isotropic dimer model for $S=3/2$ ions with the inclusion of inter-dimer interactions (θ). The parameters are $g=2.52$, $J=-14.8\ \mathrm{cm}^{-1}$, $\theta=-0.9$ K, assuming a 7% contribution from paramagnetic impurities. The small θ value corresponds to a very weak antiferromagnetic exchange coupling through the pyrazine bridge, which is in agreement with the result obtained for **2**.

In summary, three new cobalt vanadate compounds have been synthesized by employing 4,4′-bipy, pz and 2-pzc bridging ligands. The first contains only cyclic V_4O_{12} tetramers, whereas the latter two involve metavanadate chains. All three are thermally stable up to >300 °C. It can be concluded that the combination of a vanadium oxide backbone increases the thermal stability of metal–organic coordination polymers and that the pyrazine ligand has a suitable size to form a coordination polymer without destroying the metavanadate chain. Syntheses of related compounds containing the metavanadate backbone by the modification of pyrazine ligand are anticipated. By using the 2-pyrazinecarboxylate ligand, we have succeeded in synthesizing not only **3** with a framework structure, but also two related compounds with a novel chiral open-framework structure.[21] The frameworks of the latter two are stable up to 400 °C.

Acknowledgements

We thank the National Science Foundation (DMR-9805881) and the R. A. Welch Foundation for financial support. This work made use of MRSEC/TCSUH Shared Experimental Facilities supported by the National Science Foundation under Award number DMR-9632667 and the Texas Center for Superconductivity at the University of Houston.

References

1 M. T. Pope, 'Polyoxoanions', in *Encyclopedia of Inorganic Chemistry*, R. B. King, ed., John Wiley, New York, 1994, vol. 6.

2 A. S. J. Wéry, J. M. Gutiérrez-Zorrilla, A. Luque, M. Ugalde and P. Román, *Chem. Mater.*, 1996, **8**, 408.

3 Y. Zhang, P. J. Zapf, L. M. Meyer, R. C. Haushalter and J. Zubieta, *Inorg. Chem.*, 1997, **36**, 2159.

4 L.-M. Zheng, J.-S. Zhao, K.-H. Lii, L.-Y. Zhang, Y. Liu and X.-Q. Xin, *J. Chem. Soc., Dalton Trans.*, 1999, 939.

5 R. L. LaDuca Jr., C. Brodkin, R. C. Finn and J. Zubieta, *Inorg. Chem. Commun.*, 2000, **3**, 248.

6 S. Aschwanden, H. W. Schmalle, A. Reller and H. R. Oswald, *Mater. Res. Bull.*, 1993, **28**, 45.

7 J. R. D. DeBord, Y. Zhang, R. C. Haushalter, J. Zubieta and C. J. O'Connor, *J. Solid State Chem.*, 1996, **122**, 251.

8 R. L. LaDuca Jr., R. Finn and J. Zubieta, *Chem. Commun.*, 1999, 1669.

9 P. J. Hagrman, C. Bridges, J. E. Greedan and J. Zubieta, *J. Chem. Soc., Dalton Trans.*, 1999, 2901.

10 Y. Zhang, J. R. D. DeBord, C. J. O'Connor, R. C. Haushalter, A. Clearfield and J. Zubieta, *Angew. Chem., Int. Ed. Engl.*, 1996, **35**, 989.

11 X. Wang, L. Liu, A. J. Jacobson and K. Ross, *J. Mater. Chem.*, 1999, **9**, 859.

12 Z. Shi, L. Zhang, G. Zhu, G. Yang, J. Hua, H. Ding and S. Feng, *Chem. Mater.*, 1999, **11**, 3565.

13 O. Kahn, *Molecular Magnetism*, VCH Publishers, Inc., New York, 1993.

14 SAINT, Program for Data Extraction and Reduction, Siemens Analytical X-ray Instruments Inc., Madison, WI, 1994–1996.

15 G. M. Sheldrick, SADABS, Program for Siemens Area Detector Absorption Corrections, University of Göttingen, Germany, 1997.

16 G. M. Sheldrick, SHELXTL, Program for Refinement of Crystal Structures, Siemens Analytical X-ray Instruments Inc., Madison, WI, 1994.

17 J. Lu, T. Paliwala, S. C. Lim, C. Yu, T. Niu and A. J. Jacobson, *Inorg. Chem.*, 1997, **36**, 923.

18 L.-M. Zheng, X. Wang and A. J. Jacobson, *J. Solid State Chem.*, 2000, **152**, 174.

19 A. Escuer, R. Vicente, B. Mernari, A. E. Gueddi and M. Pierrot, *Inorg. Chem.*, 1997, **36**, 2511.

20 T. Ishida, S. Mitsubori, T. Nogami and H. Iwamura, *Mol. Cryst. Liq. Cryst. Sci. Technol., Sect. A*, 1993, **233**, 345.

21 L.-M. Zheng, T. Whitfield, X. Wang and A. J. Jacobson, *Angew. Chem., Int. Ed.*, 2000, **39**, 4528.